

Oligomerization of the UapA Purine Transporter Is Critical for ER-Exit, Plasma Membrane Localization and Turnover

Olga Martzoukou¹, Mayia Karachaliou¹, Vassilis Yalelis¹, James Leung², Bernadette Byrne², Sotiris Amillis¹ and George Diallinas¹

¹ - Faculty of Biology, University of Athens, Panepistimioupolis 15784, Athens, Greece

² - Division of Molecular Biology, Imperial College, London SW7 2AZ, UK

Correspondence to George Diallinas: diallina@biol.uoa.gr

<http://dx.doi.org/10.1016/j.jmb.2015.05.021>

Edited by I. B. Holland

Abstract

Central to the process of transmembrane cargo trafficking is the successful folding and exit from the ER (endoplasmic reticulum) through packaging in COPII vesicles. Here, we use the UapA purine transporter of *Aspergillus nidulans* to investigate the role of cargo oligomerization in membrane trafficking. We show that UapA oligomerizes (at least dimerizes) and that oligomerization persists upon UapA endocytosis and vacuolar sorting. Using a validated bimolecular fluorescence complementation assay, we provide evidence that a UapA oligomerization is associated with ER-exit and turnover, as ER-retained mutants due to either modification of a Tyr-based N-terminal motif or partial misfolding physically associate but do not associate properly. Co-expression of ER-retained mutants with wild-type UapA leads to *in trans* plasma membrane localization of the former, confirming that oligomerization initiates in the ER. Genetic suppression of an N-terminal mutation in the Tyr motif and mutational analysis suggest that transmembrane α -helix 7 affects the oligomerization interface. Our results reveal that transporter oligomerization is essential for membrane trafficking and turnover and is a common theme in fungi and mammalian cells.

© 2015 Elsevier Ltd. All rights reserved.

Introduction

In eukaryotes, polytopic transmembrane proteins, such as transporters, channels and receptors, are co-translationally integrated in the ER (endoplasmic reticulum) membrane and subsequently follow a vesicular secretory pathway for targeting to their final destination, this being the plasma or organellar membranes [1,2]. Central to the process of transmembrane protein exit from the ER is the concentrative packaging of protein cargoes in cytoplasmically budding COPII vesicles [3–8]. Assembly of the COPII coat on the ER membrane occurs in a stepwise fashion, beginning with recruitment of the GTPase Sar1, which recruits the heterodimeric Sec23/24. The Sec23/24 makes additional interactions directly with the membrane. Sec24 serves as the principle cargo binding adaptor. Following pre-budding complex formation, heterodimers of Sec13/31 are recruited via interaction between Sec23 and Sec31, and this interaction drives membrane curvature. In addition to

the need for proper cargo folding [7,9,10], the process of ER-exit also requires the presence of specific ER-exit motifs on the cytoplasm-facing side of cargo proteins, usually in their N- or C-terminal region. Such short motifs include di-basic, tri-basic, di-acidic, di-leucine or tyrosine-based signals, several of which interact with the Sec23p–Sec24p complex in a Sar1p-dependent way [3,11–14]. Disruption of these motifs, similar to cargo misfolding, leads to ER retention. After vesicle formation, downstream events lead to uncoating of transport vesicles and recycling of the COPII coat components [4,8]. COPII vesicle membrane cargoes are sorted in the *cis*-Golgi and eventually in the *trans*-Golgi network, an important sorting station where cargoes are packaged into distinct transport vesicles and eventually targeted to various membrane destinations [15]. Although our understanding of COPII-mediated vesicle formation has developed substantially over the past two decades, many details of this process remain unresolved.

The short cargo motifs required for ER-exit are believed to interact mainly with one of three binding sites on the COPII coat component, Sec24 [16]. The majority of ER-exported membrane proteins, however, carry no known export signal in their sequence. Thus, either new signals remain to be identified or something else drives their recruitment into COPII vesicles. As many membrane proteins form oligomers prior to export from the ER, combinatorial signals have been postulated to link oligomerization to efficient export [17]. For a yeast COPII binding cargo receptor protein and its mammalian homologue (Emp47p, a type I membrane protein), oligomerization is required for its export from the ER but is not required for efficient binding of COPII subunits in the pre-budding complex [18]. This shows that oligomerization acts downstream from the cargo–Sec24 interaction. Very recently, Springer *et al.* showed that regulated oligomerization induces the packaging of a membrane protein into COPII vesicles independently of any putative ER-exit motif [19]. Oligomerization or assembly of cargo proteins seems important for ER-exit of some other cargo proteins, including SNARE molecules or G-protein-coupled receptors [20–22]. Oligomerization of neurotransmitter (e.g., dopamine and serotonin) transporters has also been shown to occur in the ER and is maintained both at the cell surface and during trafficking between the plasma membrane and endosomes [23–30]. The human blood–brain barrier glucose transport protein GLUT1 also forms homodimers and homotetramers in detergent micelles and in cell membranes, which in turn seems to determine its function [31].

In this work, we use the *Aspergillus nidulans* purine transporter UapA as a model transmembrane cargo to investigate the role of cargo oligomerization in ER-exit, plasma membrane localization and turnover. UapA is an H⁺/uric acid-xanthine symporter consisting of 14 transmembrane segments (TMS) and cytoplasmic N- and C-termini. It is the founding member of the ubiquitously conserved Nucleobase-Ascorbate Transporter family [32–34]. The choice of UapA follows from the uniquely detailed current knowledge of its structure, function and regulation of expression, together with preliminary genetic evidence suggesting that UapA might oligomerize [35]. Inactive UapA mutants, unlike active wild-type UapA, cannot be endocytosed in response to substrate transport but can do so when co-expressed with active UapA. The simplest explanation for this phenomenon, called *in trans* endocytosis, is that UapA molecules oligomerize (at least dimerize) in the plasma membrane so that it is sufficient to have only a fraction of active molecules to recruit or activate the endocytic machinery and thus internalize both active and non-active UapA molecules [35,36]. Here, we provide multiple lines of evidence that UapA dimerizes (oligomerizes) in the ER membrane and

provide evidence for a link among oligomerization, ER-exit and subsequent membrane trafficking. Our results are discussed in relation to similar findings concerning the role of oligomerization of mammalian transporters.

Results

Biophysical evidence for UapA dimerization

We have recently isolated a specific mutant with exceptional stability for performing biophysical studies [37]. This mutant has a missense mutation replacing a Gly with a Val residue in TMS10, in addition to a deletion removing the first 11 N-terminal amino acids. A GFP-tagged version of UapA-G411VΔ1-11 is normally secreted and localized in the plasma membrane of *A. nidulans* or *Saccharomyces cerevisiae* (data not shown). The mutant exhibits highly reduced transport activity but retains substrate binding, strongly indicating that the gross folding of the transporter is not significantly affected [38]. UapA-G411VΔ1-11 was purified after heterologous expression in *S. cerevisiae* and used in static light-scattering measurements. As shown in Fig. 1, the measured molecular mass for UapA-G411VΔ1-11 is 140 ± 4.2 kDa. Given that the predicted molecular mass of the monomeric form of UapA-G411VΔ1-11 is 60,138 kDa, our data support that UapA can form dimers.

In vivo indirect evidence for UapA oligomerization in the plasma membrane

We have shown before that endocytosis of non-active UapA molecules occurs when these are co-expressed with active UapA molecules. This phenomenon of *in trans* endocytosis occurs even when the active UapA molecule cannot, by itself, be endocytosed due to the presence of mutation Lys572Arg, which prevents Hula/ArtA-dependent ubiquitination [35,36]. To further investigate whether the non-ubiquitylated mutant version UapA-K572R can be itself endocytosed *in trans* when expressed with active UapA molecules, we constructed a GFP-tagged UapA-K572R (UapA-K572R-GFP) and expressed it in a genetic background that hyper-expresses untagged wild-type UapA molecules due to a promoter mutation [39]. Results in Fig. 2 show that UapA-K572R-GFP is efficiently internalized upon imposing endocytic conditions (ammonium or uric acid addition), solely when co-expressed with wild-type UapA molecules. As UapA-K572R-GFP is a non-ubiquitylated version of UapA and ubiquitination is absolutely necessary for endocytosis, the most rational explanation for our results is that the mutant molecules are internalized due to their tight dimerization/oligomerization with wild-type UapA molecules.

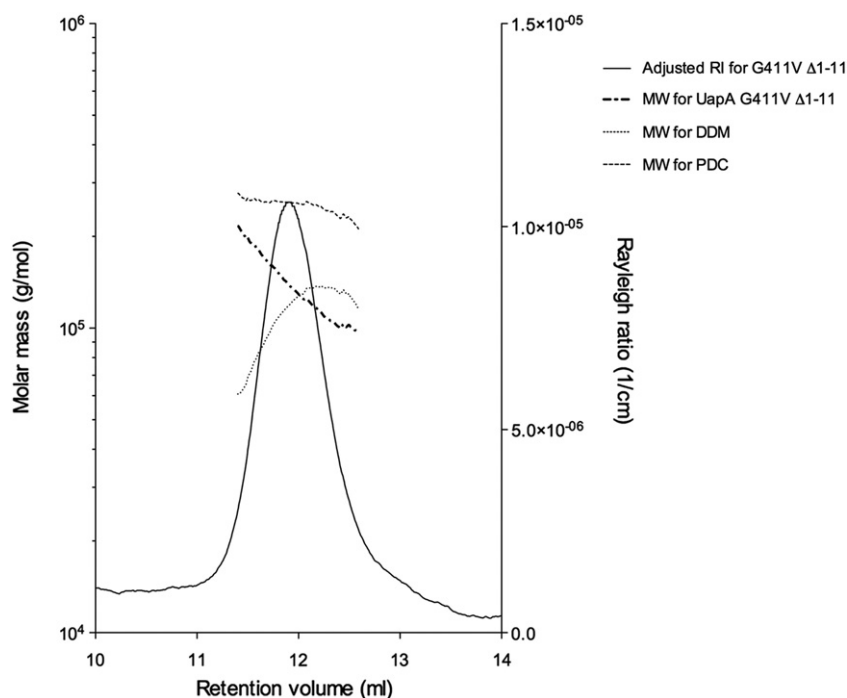


Fig. 1. Light-scattering measurements of purified UapA-G411V Δ 1-11. The measurements from the refractive index detector for UapA-G411V Δ 1-11 and the DDM micelle are indicated in black broken and dotted lines, respectively. The measurements from the refractive index detector for the total protein–detergent micelle are shown in the gray broken line. The measured molecular mass for UapA-G411V Δ 1-11 is 140 ± 4.2 kDa. The predicted molecular mass of the monomeric form of UapA-G411V Δ 1-11 is 60,138 kDa. The data strongly suggest that the UapA is dimeric in DDM solution.

BiFC assays support UapA oligomerization

Bimolecular fluorescence complementation (BiFC), as well as its version referred to as split-YFP assay, allows the *in vivo* detection of oligomerization through reconstitution of a fluorescent protein that has previously been bisected [40]. Here, we used this system to investigate further UapA dimerization/oligomerization *in vivo*. We constructed three isogenic strains, two expressing UapA-tagged C-terminally with either the N-terminal or the C-terminal part of YFP (UapA-YFP_N and UapA-YFP_C, respectively) and one co-expressing UapA-YFP_N and UapA-YFP_C, simultaneously. Co-expression of UapA-YFP_C and UapA-YFP_N in a strain lacking endogenous uric acid transporters (*uapAΔ uapCΔ*) resulted in growth on uric acid, sensitivity to substrate analogues (oxypurinol and 2-thioxanthine) (Fig. 3a) and prominent reconstitution of YFP fluorescence in the plasma membrane (Fig. 3b). In contrast, no significant YFP fluorescence signal was detected when the two halves of YFP were expressed as separate fusions with UapA (Fig. 3b).

To our knowledge, BiFC has not been used before as an assay for oligomerization of polytopic membrane proteins. Thus, one might argue that reconstitution of fluorescent YFP is not a formal proof for oligomerization but might rather reflect proximal

localization of proteins restricted in the environment of the plasma membrane. As shown later in this manuscript, evidence against this argument comes from experiments showing that specific mutant versions of UapA do not reconstitute split-YFP in analogous assays. For further reinforcing the validity of the BiFC assays for detecting UapA oligomerization, we adapted the BiFC experiment for detecting possible interactions of UapA with another plasma membrane transporter, namely, the L-proline transporter PrnB [41]. We co-expressed UapA-YFP_N with PrnB-YFP_C (see Materials and Methods) and tested for YFP reconstitution, as previously described. The right panel in Fig. 3b shows that no fluorescence was obtained, strongly supporting the idea that YFP reconstitution via UapA molecules reflects a specific association, most evidently dimerization.

In the experiments shown in Fig. 3, UapA-YFP expression was driven by the native *uapA* promoter, which allows continuous and relatively low level UapA synthesis. We also constructed analogous strains where the expression of UapA-YFP_C and UapA-YFP_N was driven by the controllable *alcA_p* promoter [42]. The *alcA_p*-UapA-YFP_C/*alcA_p*-UapA-YFP_N strain could grow on uric acid, similarly to a control strain expressing *alcA_p*-UapA-GFP (Fig. 3c). This is also reflected in very similar xanthine transporter rates

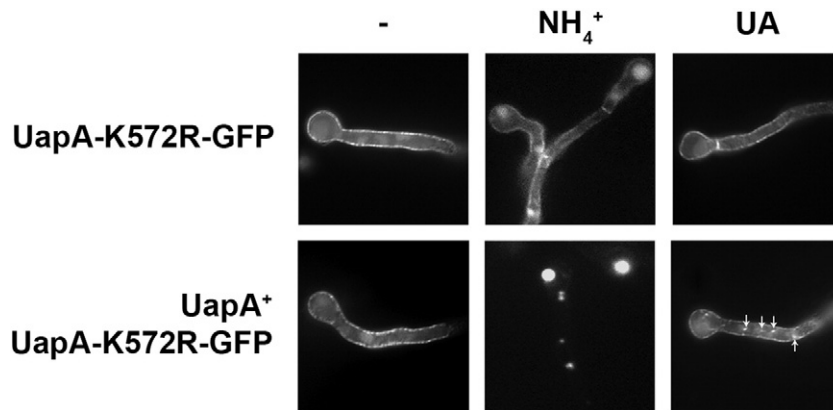


Fig. 2. *In trans* endocytosis of a non-ubiquitinated UapA mutant co-expressed with wild-type UapA. UapA-K572R-GFP is a UapA mutant that cannot be ubiquitinated and endocytosed in response to ammonium or substrate (UA; uric acid) addition in the growth medium. The figure shows an epifluorescence microscopy analysis of a strain expressing UapA-K572R-GFP alone or co-expressed with wild-type UapA in the genetic background of *uapA100*. *uapA100* is a promoter mutation leading to a 3-fold increase in UapA protein levels. The subcellular localization of UapA-K572R-GFP is followed under control conditions and endocytic conditions (ammonium or UA addition). Arrows indicate the vacuolar staining of UapA-K572R-GFP.

in the two strains (Fig. 3d). Most importantly, a strong YFP signal was observed, associated with the plasma membrane in the strain co-expressing *alcA_p-UapA-YFP_C* and *alcA_p-UapA-YFP_N*, solely under inducing conditions for *alcA_p*, (0.1% fructose, ethanol for 4 h). Under repressing conditions (1% glucose for 3 h), no YFP fluorescence was visible (Fig. 3e). The reconstitution of YFP when attached to separate UapA molecules suggests that UapA dimerizes so that the C-tails of the two monomers are in close distance necessary to reconstitute YFP.

We also tested whether UapA-YFP_N/UapA-YFP_C apparent oligomerization, shown by reconstitution of YFP, persists upon endocytosis. Figure 3f shows that UapA-YFP_N/UapA-YFP_C internalization is evident in the presence of NH₄⁺ or excess substrate. In the presence of ammonium, YFP fluorescence is still associated with the plasma membrane but is also visible in large vacuoles (detected by CMAC). Diffuse low fluorescence is apparent within the vacuolar lumen, which suggests that the two parts of YFP dissociate upon turnover of UapA. In the presence of substrate (uric acid), UapA internalization is also evident in addition to motile early endosomes and small vacuoles, as has been shown previously for wild-type UapA-GFP [35]. These results show that UapA dimerization persists during endocytosis, in early endosomes and all along the endosomal pathway until internalization into the vacuolar lumen.

Pull-down assays support UapA oligomerization

To provide further direct evidence for UapA oligomerization, we also performed pull-down assays using membrane protein extracts of a strain co-expressing differentially tagged UapA molecules. A strain co-

expressing from the *alcA_p* promoter GFP- and His₁₀-tagged versions of UapA was constructed. Protein samples were purified with a Ni-NTA column under non-denaturing conditions and the eluted fractions were analyzed by SDS polyacrylamide gel silver staining (Fig. 4a, left panel). Western blot analysis with anti-His antibody identified, in the eluted fractions at 250 mM imidazole, a major band at ~55 kDa, which corresponds to monomeric UapA-His [43]. A second minor band of estimated size close to 110 kDa, probably corresponding to UapA-His dimers, was also evident (Fig. 4a). Western blot analysis of the eluted UapA-specific fraction with anti-GFP antibody showed a prominent band migrating at the position corresponding to monomeric UapA-GFP (~75 kDa), thus demonstrating that UapA-GFP co-purified with UapA-His, very probably as a result of dimerization (Fig. 4b). This is further confirmed in the negative control strain where UapA-GFP is expressed without UapA-His. In this case, the eluted imidazole fraction (250 mM) from a Ni-NTA column does not contain UapA-GFP. A very similar result was obtained with an inverse pull-down assay where UapA-GFP was first precipitated with anti-GFP antibodies on ProtA-Sepharose beads, followed by co-immunoprecipitation of UapA-His detected with anti-His antibody, confirming the dimerization/oligomerization of UapA molecules (see Supplementary Fig. S1).

The data shown in Fig. 4a and b were obtained using protein expressed from the *alcA_p* promoter induced with ethanol for 4 h before collecting total membrane protein extracts. This means that UapA molecules are continuously synthesized so that, in addition to the plasma membrane, UapA is also localized in the ER, the Golgi and trafficking vesicles. We repeated the pull-down experiment with protein

extracts isolated after repression of *de novo* UapA synthesis. Under these conditions, detectable UapA-GFP molecules are solely associated with the plasma membrane [44]. Results in Fig. 4c were practically identical with those of Fig. 4b supporting that UapA-His/UapA-GFP dimerization persists in the plasma membrane. Under these conditions, we again obtained, besides monomeric UapA species, additional higher molecular weight (MW) bands, which might represent dimers/oligomers or aggregates of UapA-GFP that are SDS resistant.

We also tested whether the presence of substrates during growth affects the apparent UapA-His/UapA-GFP dimerization. Figure 4d shows no effect of substrate on the pull-down result. This is in line with the results in Fig. 3f, which showed that apparent UapA dimers persist during internalization and until turnover in the vacuolar lumen. The reduced amount of both UapA-His and UapA-GFP after prolonged presence of substrate is probably due to internalization and the subsequent vacuolar turnover [35].

Identification of a cytoplasmic N-terminal signal necessary for ER-exit of UapA

ER retention of polytopic membrane proteins is usually due to partial misfolding or the lack of functional ER-exit signals. To identify possible ER-exit signals in UapA, we carried out a systematic mutational analysis of the N-terminal cytoplasmic region of UapA-GFP. This segment that is 68 amino acids long is the most likely location of ER-exit and trafficking motifs, as deletion of the cytoplasmic C-terminal region has absolutely no effect in these processes [35]. Deletions and Ala scanning mutagenesis revealed a short sequence (Asp44-Tyr45-Asp46-Tyr47) and particularly a single residue within it, Tyr47, as being critical for ER-exit and thus essential for detectable UapA transport activity and growth on uric acid (Fig. 5). Substitution of the entire Asp-Tyr-Asp-Tyr sequence with Ala residues (DYDY₄₇/A₄) leads to dramatic turnover of UapA associated with retention in perinuclear ER membranes. This effect seems to be mainly due to replacement of Tyr47, as the single mutation Y47A leads to a similar effect to that seen for the quadruple DYDY₄₇/A₄ mutant. Importantly, direct transport assays showed that over-expressed UapA-Y47A conserves a normal K_m value for physiological substrates (see Fig. 5d). This is highly suggestive that the gross folding of the UapA-Y47A polypeptide is not affected. In turn, this confirms that reduced ER-exit and increased turnover in this mutant are not due to misfolding.

To further understand the nature of the defect in Y47A, we made systematic substitutions of Tyr47 and showed that Tyr can be functionally substituted with Phe, but not with other residues (Fig. 5e). Thus, the presence of an aromatic amino acid at position 47 is necessary for proper ER-exit and expression

in the plasma membrane of UapA. The Asp-Tyr-Asp-Tyr consensus sequence, including Tyr47, is highly conserved in all fungal homologues of UapA (Fig. S2).

ER-retained mutants of UapA physically associate but do not reconstitute split-YFP

We investigated whether mutations affecting ER-exit also affect oligomerization. To that end, we used three UapA mutant versions. The first two, UapA-I74D and UapA- Δ TMS14, were examples of partially misfolded mutants [45,46]. The third is UapA-DYDY₄₇/A₄, as described above. We used UapA-DYDY₄₇/A₄ rather than the UapA-Y47A, as ER-exit is more drastically affected in this mutant than in UapA-Y47A.

We performed BiFC assays for UapA-I74D, UapA- Δ TMS14 and UapA-DYDY₄₇/A₄, as described for wild-type UapA. All strains made (see Materials and Methods) had the expected growth phenotypes (Fig. S3). None of the mutants tested showed significant YFP reconstitution, strongly suggesting that all relevant mutation impair dimerization/oligomerization (Fig. 6a). In apparent contradiction with the BiFC assays, pull-down assays showed that mutant molecules of UapA-DYDY₄₇/A₄ or UapA-I74D physically associate (Fig. 6b). However, in UapA mutants, it is evident that the amount of monomeric UapA-GFP co-precipitated is relatively reduced, in favor of an increase in a high MW signal, when compared with the analogous ratio in the wild-type control. Although the quantification of monomeric to higher MW oligomers or aggregates in different strains is difficult to estimate rigorously, mainly due to different half-lives of wild-type and mutant UapA molecules, in light of the BiFC assays, our results strongly support the idea that the physical association in the mutants is topologically different from the interaction in the wild-type UapA.

In trans exocytosis of ER-retained UapA mutants supports early oligomerization in the ER

We performed BiFC assays using strains in which the mutant versions of UapA (UapA-I74D-YFP_C, UapA- Δ TMS14-YFP_C or UapA-DYDY₄₇/A₄-YFP_C) were co-expressed with a wild-type UapA (UapA-YFP_N). In all cases, the strains grew well on uric acid, showing that there was no dominant negative effect of the mutant version on the wild-type UapA (Fig. 7a). Figure 7b shows that YFP fluorescence is reconstituted in UapA-I74D-YFP_C/UapA-YFP_N and UapA-DYDY₄₇/A₄-YFP_C/UapA-YFP_N, but not in UapA- Δ TMS14-YFP_C/UapA-YFP_N. Most importantly, fluorescence is associated with the plasma membrane. The reconstitution of split-YFP shows that UapA-I74D-YFP_C or UapA-DYDY₄₇/A₄-YFP_C molecules are able to dimerize or physically associate with wild-type UapA

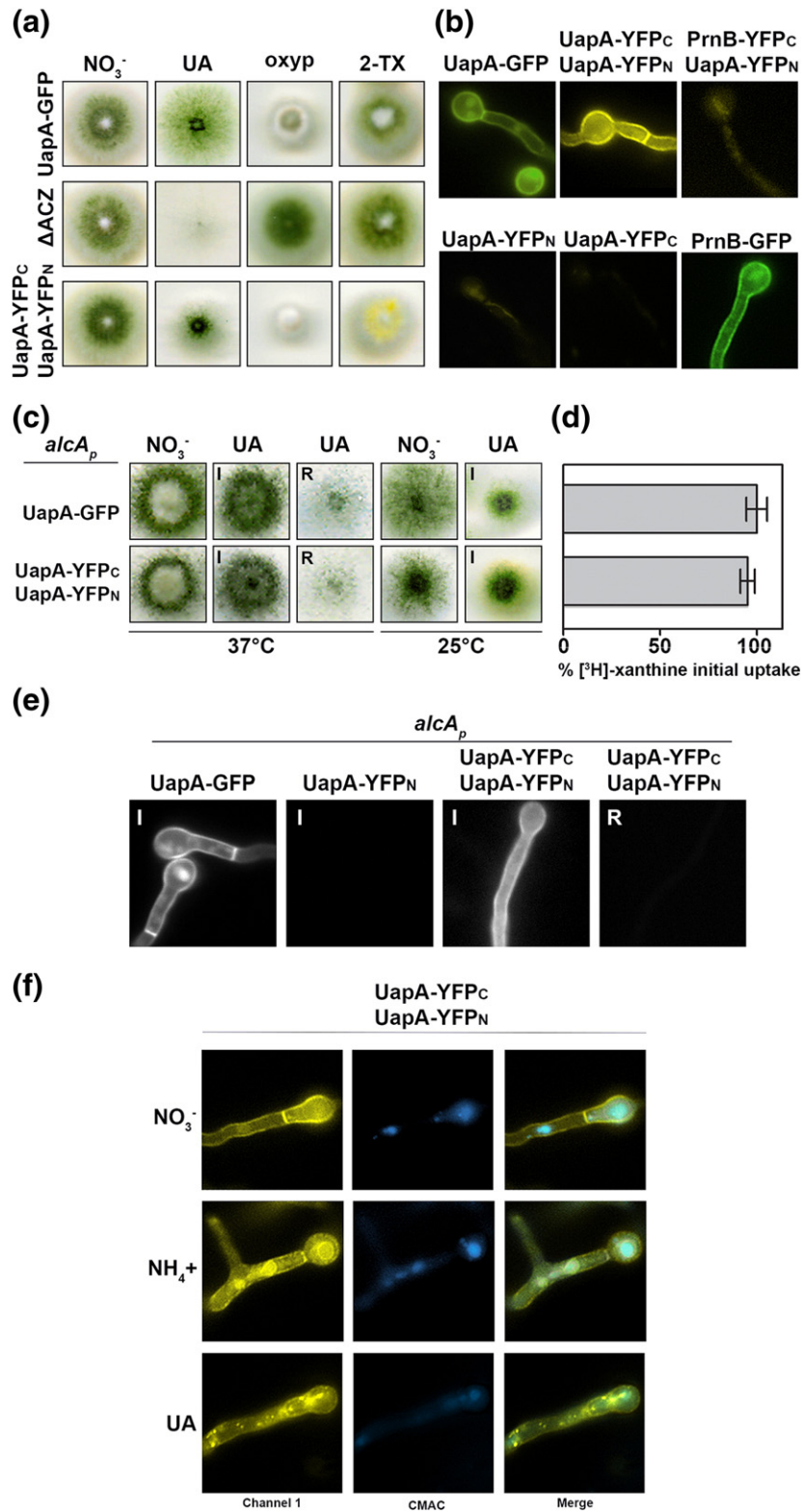


Fig. 3. (legend on next page)

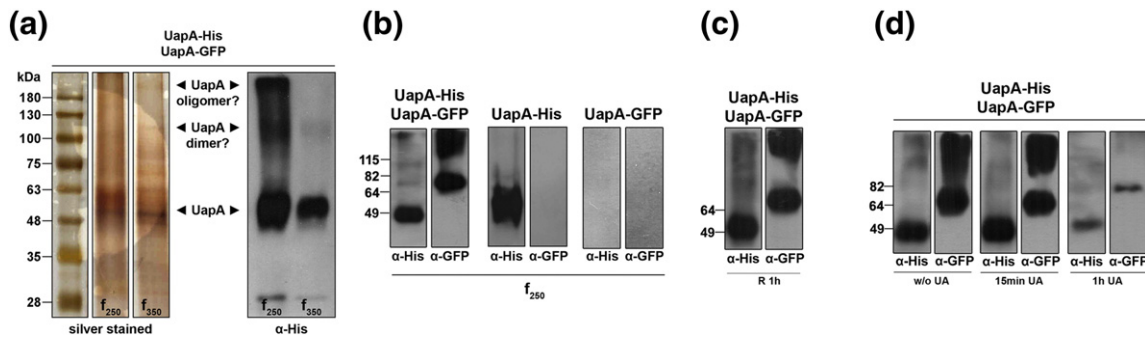


Fig. 4. Direct biochemical evidence for UapA oligomerization in a strain co-expressing UapA-His₁₀ and UapA-GFP. (a) Solubilized total membrane protein preparations from the strain co-expressing UapA-His₁₀ and UapA-GFP under inducing conditions were applied to Ni-NTA columns, eluted with increasing concentrations of imidazole (only f₂₅₀ and f₃₅₀ fractions are shown) and analyzed by SDS polyacrylamide gel electrophoresis, followed by silver staining or immunoblotting with an anti-His antibody. A prominent band reacting with the anti-His antibody in the fraction eluted at 250 mM is detected. The size of this band is estimated to be ~55 kDa, which corresponds to monomeric UapA-His [43]. A less prominent anti-His specific band appearing at just over the 100 kDa might correspond to a dimeric form of UapA. (b) The f₂₅₀ fraction of the strain co-expressing UapA-His and UapA-GFP also reacts with the anti-GFP. In contrast, the same fraction from a strain expressing solely UapA-His does not react with the anti-GFP antibody, as expected. (c) Western blot analysis, using anti-GFP antibody, of similarly eluted UapA-His fractions isolated from the UapA-His₁₀/UapA-GFP strain grown under repressing conditions (1 h glucose). Under this condition, *de novo* synthesis is blocked and thus preformed UapA molecules are solely present in the plasma membrane. (d) Western blot analysis, using anti-GFP antibody, of eluted UapA-His fractions isolated from the UapA-His₁₀/UapA-GFP strain incubated for 4 h under inducing conditions, in the presence of substrate (uric acid) for 15 min or 1 h before cell harvesting. In all cases, protein samples are heated at 37 °C for 30 min before loading onto the SDS-PAGE gel.

molecules. In UapA-DYDY₄₇/A₄-YFP_C/UapA-YFP_N, fluorescence is also visibly associated with perinuclear ER membrane rings. This confirms that oligomerization occurs in the ER membrane and persists in the plasma membrane. The absence of YFP reconstitution in UapA-ΔTMS14-YFP_C/UapA-

YFP_N was to be expected, as the deletion of the last transmembrane domain (TMS14) should orientate the C-terminus toward the extracellular side of the membrane, thus preventing its association with the C-terminus of wild type. Thus, the UapA-ΔTMS14-YFP_C/UapA-YFP_N experiment also serves as a

Fig. 3. *In vivo* evidence for UapA oligomerization using BiFC. (a) Growth test of the UapA-YFP_C/UapA-YFP_N transformant, as compared to a control strain expressing UapA-GFP and a mutant lacking all major purine transporters (ΔACZ). All strains shown are otherwise isogenic and thus grow similarly on standard nitrogen sources (e.g., NaNO₃). Strains expressing a functional UapA grow on uric acid (UA) as sole nitrogen source and are sensitive to oxypurinol (OX) or 2-thioxanthine (2-TX) (green/yellowish conidiospores), whereas the mutant lacking UapA shows very leaky growth on UA and is resistant to OX and 2-TX (green conidiospores). The growth profile of UapA-YFP_C/UapA-YFP_N is compatible with a functional UapA and in fact shows higher expression of UapA compared to UapA-GFP, as judged mostly by increased sensitivity to OX and 2-TX. Given that the single chimeric transporter UapA-YFP_C or UapA-YFP_N is also functional (results not shown), the YFP tags do not affect, within the limit of growth tests, UapA function. Strains are grown at 25 °C. (b) Epifluorescence microscopic analysis of the strains expressing either UapA-YFP_C or UapA-YFP_N, or co-expressing UapA-YFP_C/UapA-YFP_N, compared to an isogenic strain expressing UapA-GFP. Strains co-expressing UapA-YFP_N/PmB-YFP_C, grown on proline, are also shown as a negative control. (c and d) Growth test and radiolabeled [³H]xanthine transport activity of a strain co-expressing *alcA_p*-UapA-YFP_C/*alcA_p*-UapA-YFP_N. The panel on the left confirms that the *alcA_p*-UapA-YFP_C/*alcA_p*-UapA-YFP_N strain grows similarly to isogenic *alcA_p*-UapA-GFP. Notice that UapA-mediated full growth on UA is only observed under inducing conditions (I; fructose, ethanol) for the *alc_p* promoter, while only marginal growth is observed under repressing (R; glucose) conditions. The panel on the right confirms that *alcA_p*-UapA-YFP_C/*alcA_p*-UapA-YFP_N and *alcA_p*-UapA-GFP have comparable transport activities. Transport activities are expressed as % of initial uptake rate, considering the rate of UapA-GFP as 100%. Results represent averages of three experiments, each experiment carried out in triplicate, with standard deviation <20%. (e) Epifluorescence microscopic analysis of strains expressing *alcA_p*-UapA-GFP or *alcA_p*-UapA-YFP_N, or co-expressing *alcA_p*-UapA-YFP_C/*alcA_p*-UapA-YFP_N. For *alcA_p*-UapA-GFP or *alcA_p*-UapA-YFP_N strains, only inducing conditions (I; fructose, ethanol) are shown, whereas for the *alcA_p*-UapA-YFP_C/*alcA_p*-UapA-YFP_N strain, both repressing (R; glucose) and inducing (I) conditions are shown. (f) Epifluorescence microscopic analysis of strains co-expressing UapA-YFP_C/UapA-YFP_N under standard conditions (nitrate as nitrogen source) or under endocytic conditions [addition of ammonium or substrate (uric acid) for 4 h in samples grown with nitrate]. Channel 1 shows reconstitution of YFP by UapA-YFP_N/UapA-YFP_C dimerization, while CMAC staining is used for vacuole detection. Endocytosis triggered by ammonium leads to rapid sorting of UapA-YFP_N/UapA-YFP_C apparent dimers in large vacuoles, whereas substrate-triggered endocytosis results in sorting of UapA-YFP_N/UapA-YFP_C in motile early endosomes and small vacuoles.

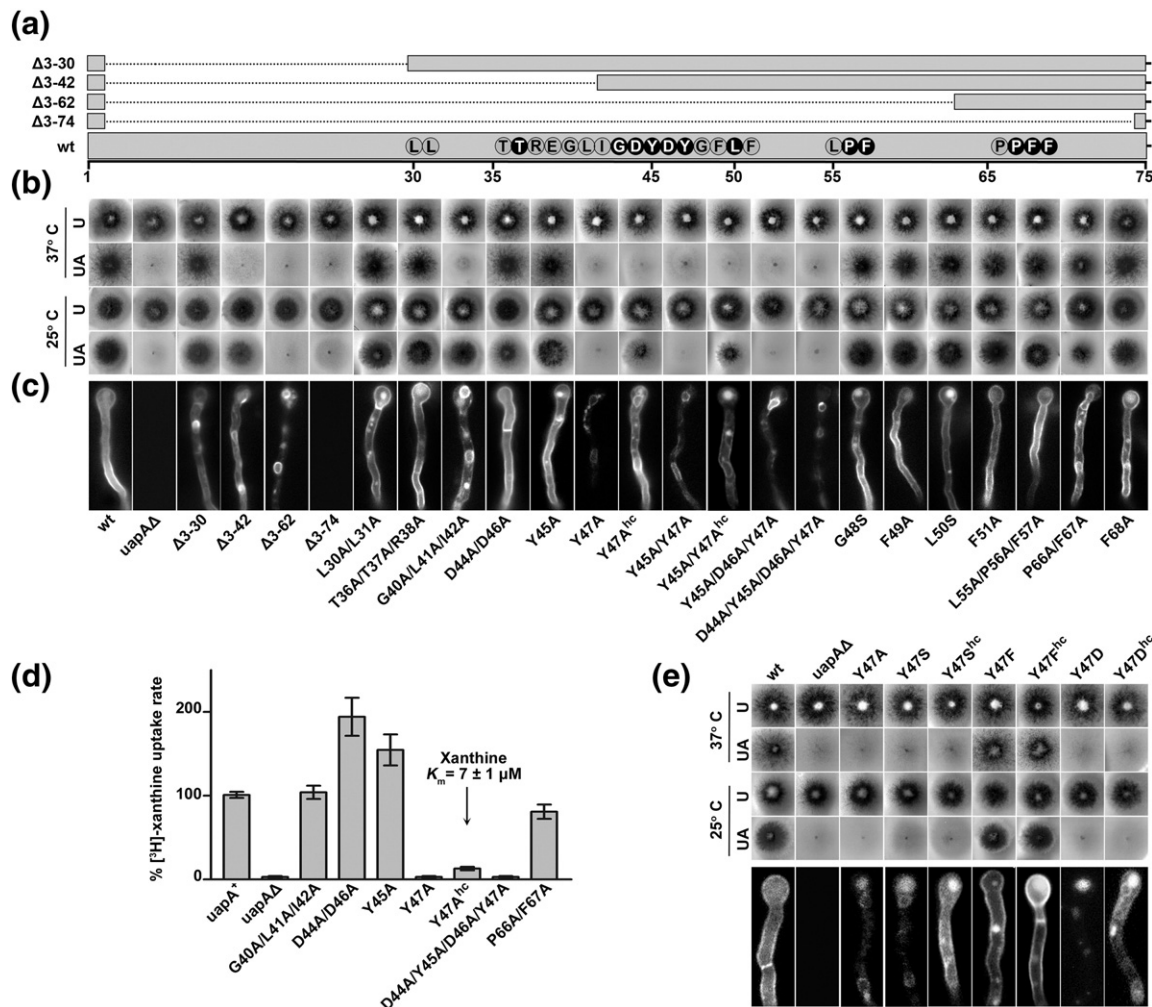


Fig. 5. Identification of an N-terminal motif necessary for ER-exit of UapA. (a) Schematic representation of the N-terminal region of UapA, highlighting the amino acid residues conserved and mutated. Overlapping deletions of the N-terminal region are also depicted. hc means expression from high-copy plasmids. (b) Growth test of N-terminal UapA mutants. All mutants shown, unless otherwise stated, arise from functional single-copy plasmid integration events. In all cases, UapA is functionally tagged with GFP. hc stands for plasmid high-copy transformants that over-express the mutant form of UapA. This constitutes a standard tool for further testing the subcellular localization and transport activity of selected mutants that are expressed at very low levels, as is the case here of Y47A. Mutants are tested on MM either with a standard nitrogen source unrelated to UapA function (urea) or on uric acid, the main physiological substrate of UapA, as sole nitrogen source, at 25 °C and 37 °C. Positive and negative controls (wt and Δ UapA) are isogenic strains expressing wild-type UapA and a strain lacking all major purine transporters (*uapAΔ uapCΔ azgAΔ*), respectively. Notice that the inability for growth on uric acid is always associated with substitution of Tyr47 or deletions removing an N-terminal part including Tyr47 (Δ 3-42, Δ 3-62 and Δ 3-74). The triple substitution G40A/L41A/I42A also led to apparent loss of UapA, but only at 37 °C. (c) Epifluorescence microscopy of N-terminal UapA mutants. Mutants with apparent ER retention, reduced localization in the plasma membrane and vacuolar sorting are always associated with substitution Y47A or the deletion of an N-terminal segment including Tyr47. Deletion Δ 3-30 shows a degree of vacuolar turnover, whereas the double substitution P66A/F67A shows partial ER retention. The deletion of the entire N-terminal region leads to no fluorescence. These results are in agreement with growth tests and uptake assays. (d) Transport activities, expressed as % of initial uptake rates, of selected mutants (see Fig. 3 legend). (e) Systematic mutational analysis of Tyr47. Growth tests and epifluorescence microscopy analysis of Tyr47 substitutions show that only substitution Y47F restores the secretion of UapA to the plasma membrane and, consequently, also restores its apparent transport activity (experimental details are as above).

negative control in BiFC assays. *In trans* sorting of UapA-DYDY_{4,7}/A₄-GFP in the plasma membrane upon co-expression with over-expressed (from a

high-copy plasmid transformant) wild-type UapA further confirmed the formation of UapA dimers (Fig. 7c).

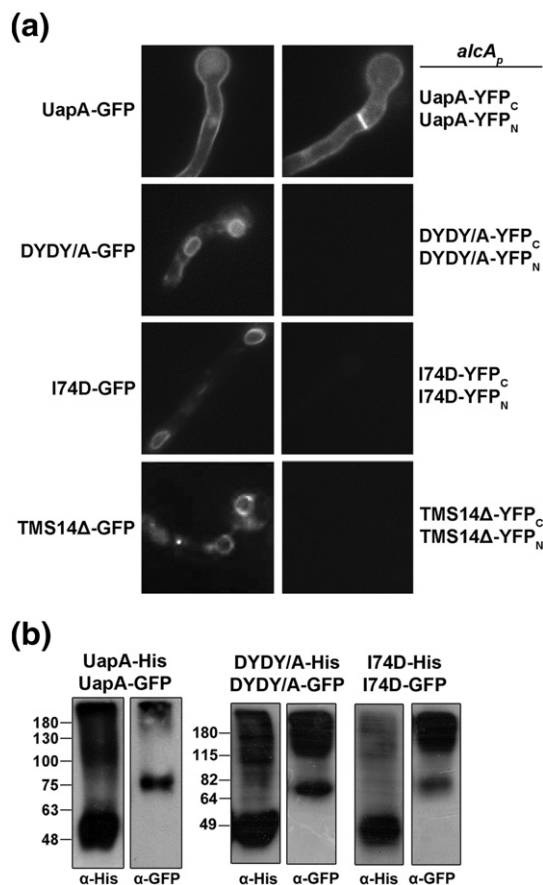


Fig. 6. UapA mutants retained in the ER do not dimerize properly. (a) BiFC assays of wild-type UapA and mutants UapA-DYDY/A₄, UapA-I74D and UapA-ΔTMS14. Strains co-expressing from the *alcA_p* promoter the mutant forms of UapA, tagged with either YFP_N or YFP_C, are shown. Isogenic strains expressing from *alcA_p* the same mutant versions UapA, or a wild-type UapA, tagged with GFP, are also included as controls. No reconstitution of YFP was detected in any of the mutants tested. (b) Pull-down experiments in strains co-expressing UapA-DYDY/A₄-GFP/UapA-DYDY/A₄-His₁₀ or UapA-I74D-GFP/UapA-I74D-His₁₀. Notice the reduced amount of monomeric co-precipitated UapA-GFP relatively to higher MW species, possibly UapA aggregates (see the text).

Genetic suppression of Y47A reveals the importance of TMS7 and TMS11 in ER-exit of UapA

We obtained two different intragenic suppressors, namely, V298A and F437C, the former restoring the defects caused by Y47A much more strongly than the latter (Fig. 8a). Val298 and Phe437 are located in the middle of TMS7 and the outward-facing end of TMS11 (Fig. 8b), respectively, both being quite well conserved residues in UapA homologues (Fig. S4). Both mutations restored UapA-mediated transport rates (Fig. 8c). Functional restoration was in line with restoration of ER-exit and plasma membrane

localization, as evidenced by both standard epifluorescence analysis and BiFC assays (Fig. 8d). Strains expressing the suppressor mutations in the absence of the original mutation (UapA-V298A or UapA-F437C) conferred growth phenotypes, subcellular localization and transport activities, similar to wild-type UapA (data not shown). Thus, suppression of Y47A is probably not due to allele-specific interactions of Tyr47 with Val298 or Phe437 but is rather a bypass of the effect of Y47A.

Gly residues in TMS7 are critical for wild-type-like oligomerization, ER-exit and turnover of UapA

Three independent observations suggested that TMS7 might be part of or affects the oligomerization interface. Firstly, the crystal structure of the bacterial UapA homologue UraA shows that TMS7 has the highest *B*-factors of all the transmembrane segments, indicating that this region of UraA is the most flexible, and therefore, it is a candidate for intermolecular interactions [47]. Secondly, TMS7 is predicted to form a bend α -helix, one part facing the lipid bilayer and the other one facing toward the TMS13 and TMS14, which are candidates for dimerization domains (Y. Alguel, A. Cameron, G. Diallinas and B. Byrne, unpublished results). Thirdly, TMS7 includes several Gly residues (Gly301, Gly305 and Gly313) in the form of GX₃G or GX₇G motifs (X being hydrophobic residues), known to be critical for inter-helical interactions in membrane proteins [48–50].

To test the importance of the Gly residues in TMS7 of UapA, we made a series of substitutions to Ala or Leu residues and functionally analyzed the corresponding mutants. In all cases, we constructed the single, double and triple substitutions. Results are shown in Fig. 9a. All substitutions to Leu, except G313L, led to apparent loss of UapA activity as judged from growth tests. In addition, none of the mutants correctly localized to the plasma membrane. Furthermore, a low UapA-GFP signal was also detected in vacuoles in several mutants. Single substitutions of Gly301, Gly305 and Gly313 to Ala did not significantly affect UapA localization and transport activity. However, double and triple substitutions scored as apparent loss-of-function mutations. In these cases, we detected dramatic vacuolar turnover and some ER retention. The fact that Ala substitutions were better tolerated than Leu substitutions was in line with observations that G/AX₃G/A or G/AX₇/A motifs can also function as weaker helical interaction motifs [48].

We tested whether UapA molecules carrying the triple Ala substitution (UapA-GGG/A₃) could dimerize. Figure 9b shows that no YFP reconstitution is obtained in strains co-expressing UapA-GGG/A₃-YFP_N and UapA-GGG/A₃-YFP_C. Relevant pull-down assays showed that, in the GGG/A₃ mutant, UapA molecules still associate despite the fact that the ratio of monomeric UapA-GGG/A₃-GFP *versus*

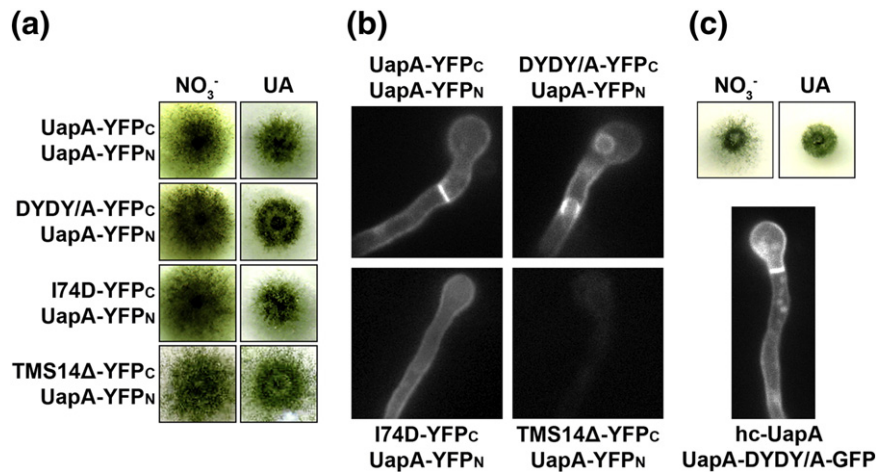


Fig. 7. *In trans* exocytosis of ER-retained UapA mutants. (a) Growth tests of strains co-expressing UapA-I74D-YFP_C, UapA-ΔTMS14-YFP_C or UapA-DYDY/A₄-YFP_C with a wild-type UapA-YFP_N. As expected, all strains grow on UA. (b) BiFC assays of the same strains shown in (a). Notice YFP fluorescence reconstitution in the plasma membrane of strains co-expressing UapA-I74D or UapA-DYDY/A₄ with wild-type UapA while there is no YFP signal detected in UapA-ΔTMS14/UapA. In UapA-DYDY/A₄/UapA, YFP signal is also detected in the perinuclear ER. (c) Growth test and epifluorescence analysis of a strain co-expressing UapA-DYDY₄₇/A₄-GFP and wild-type UapA. Notice the sorting of UapA-DYDY₄₇/A₄-GFP in the plasma membrane. In this case, the high expression of wild-type UapA (in relation to UapA-DYDY₄₇/A₄-GFP) was achieved by selecting a transformant that harbors three copies of the relative plasmid (hc-UapA).

high MW aggregates is reduced compared to wild-type UapA (Fig. 9c). Using the inverse pull-down assay where UapA-GFP is precipitated with anti-GFP antibodies on ProtA-Sepharose beads, followed by co-immunoprecipitation of UapA-His detected with anti-His, we confirmed that UapA molecules associate, but again the ratio of monomeric UapA-GGG/A₃-GFP *versus* high MW aggregates seemed somehow reduced (see Supplementary Fig. S1).

Finally, we also showed that UapA-GGG/A₃ can be sorted to the plasma membrane upon co-expression with wild-type UapA (Fig. 9d). This is in line with partial restoration of UapA-mediated growth on uric acid. Overall, the results obtained with the mutant lacking the Gly residues in TMS7 are very similar to those obtained with the other ER-retained mutants studied here (UapA-DYDY/A₄ and UapA-I74D).

Intragenic complementation of plasma membrane localization in ER-retained mutants

We also constructed strains co-expressing UapA-GGG/A₃ with UapA-DYDY/A₄-GFP and performed growth tests and epifluorescence analysis (Fig. 10). These strains could not grow on uric acid, as expected, but showed partial restoration of plasma membrane localization, never seen when these two UapA versions are expressed by themselves. This partial intragenic complementation is readily explained by dimerization, constituting further strong evidence that dimerization/oligomerization of UapA is functionally linked to ER-exit and plasma membrane localization and stability.

Discussion

Four independent assays showed that UapA forms, at least, homodimers in the ER and that oligomerization persists along the secretion pathway, in the plasma membrane and during endocytosis. Of these assays, the *in vivo* reconstitution of split-YFP proved ideal to detect minor topological changes in the association of UapA molecules. A similar strategy has been used to show transporter oligomerization in a handful of previous reports [51–55]. However, to our knowledge, this is the first time BiFC has been shown to detect highly specific transporter dimerization/oligomerization; no reconstitution of split-YFP was detected in *specific* UapA mutants or when one part of YFP was tagged in another plasma membrane transporter.

UapA, in common with most ion-driven polytopic symporters, functions as a monomer. This is based on genetic, biochemical and structural data. Although we cannot rule out that dimerization might have a subtle effect on transport kinetics *per se*, it seems much more reasonable to assume that oligomerization affects membrane trafficking, plasma membrane localization and protein stability, as proposed for several mammalian transporters (discussed also later). Recent evidence also supports the and further oligomerization of the mammalian SVCT2 vitamin C transporter, which belongs to the same protein family as UapA [56].

We examined whether UapA mutants showing problematic ER-exit associated with increased turnover can dimerize. We made use of two kinds of ER-retained

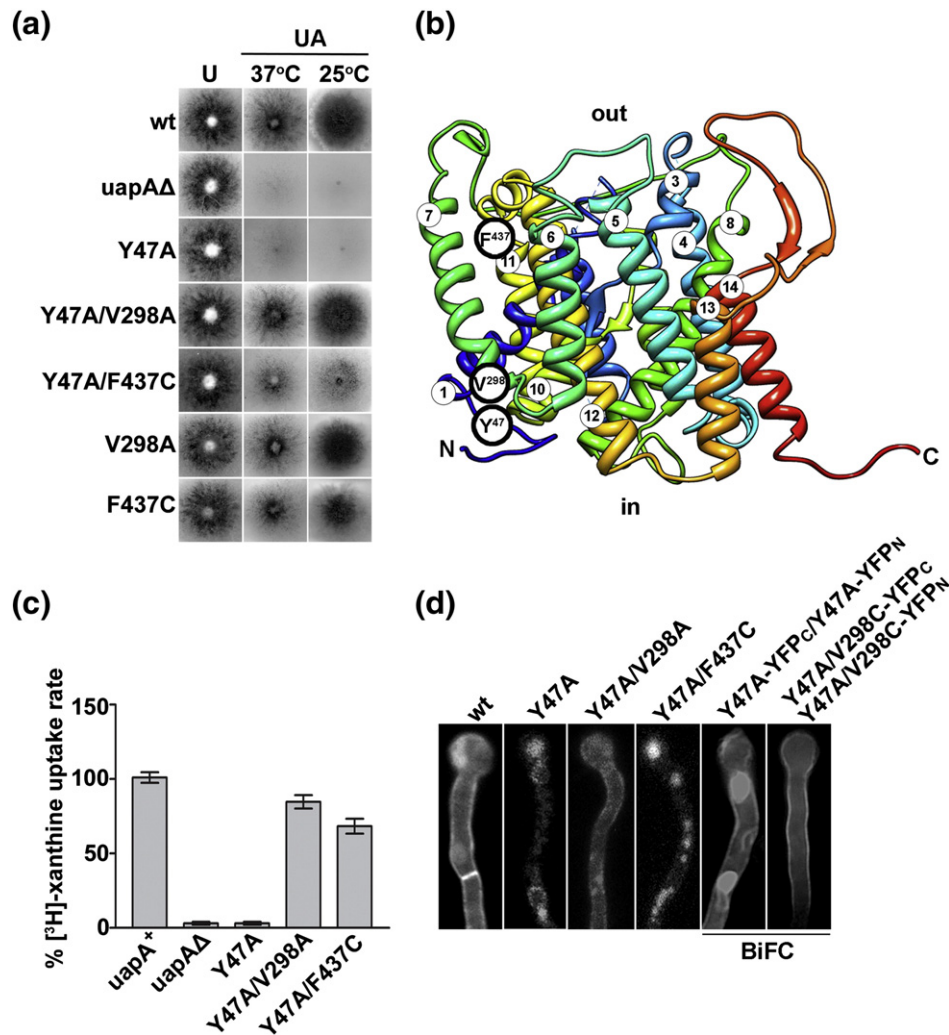


Fig. 8. Specific mutations in TMS7 and TMS11 genetically suppress the ER-exit defect of UapA-Y47A. (a) Growth tests of the two genetic suppressors compared to the original mutant. Notice that suppressor mutation V298A is stronger than F437C. (b) Identity (V298A and F437C) and topology of the two genetic suppressor mutations of UapA-Y47A. (c) Transport rates in suppressors and original mutant. (d) Epifluorescence microscopy of suppressors and original mutant and BiFC assays of UapA-Y47A and UapA-Y47A/V298A, showing the restoration of plasma membrane localization in the latter.

mutants. The first are due to partial misfolding, whereas the second are due to the lack of the N-terminal DYDY₄₇ motif, which does not seem to affect gross UapA folding. However, the two types of mutants showed similar characteristics: ER retention, increased vacuolar turnover, non-reconstitution of split-YFP fluorescence and a modified mode of association in pull-down assays. Importantly, the ER-retained mutant versions of UapA, co-expressed with wild-type UapA, were sorted in the plasma membrane. This phenomenon of *in trans* sorting seems analogous to the *in trans* endocytosis of UapA mutants, detected here (Fig. 2) and previously [35], and is most easily explained by the formation of dimers. More impressively, co-expression of different ER-retained mutants of UapA restored plasma membrane localization, which constitutes further strong evidence for dimerization (see Fig. 10).

The isolation of genetic suppressors of ER-retained mutants mapping in TMS7 and TMS11 suggested that these lipid-facing transmembrane domains of UapA [34], especially TMS7 which includes the strongest suppressor and functionally essential GX₃G motifs, must be involved in critical helical interactions. Our results strongly favor the involvement of TMS7 in homo-oligomerization. At present, we cannot propose a model on how and how many UapA monomers associate, but it seems that functional UapA association requires both helical interactions within the plasma membrane and interactions involving the cytoplasmic terminal regions of UapA. The latter interactions might in fact be crucial to the molecular cross-talk with the ER-exit machinery. Ongoing efforts to obtain the crystal structure of UapA will give a definitive answer to this issue

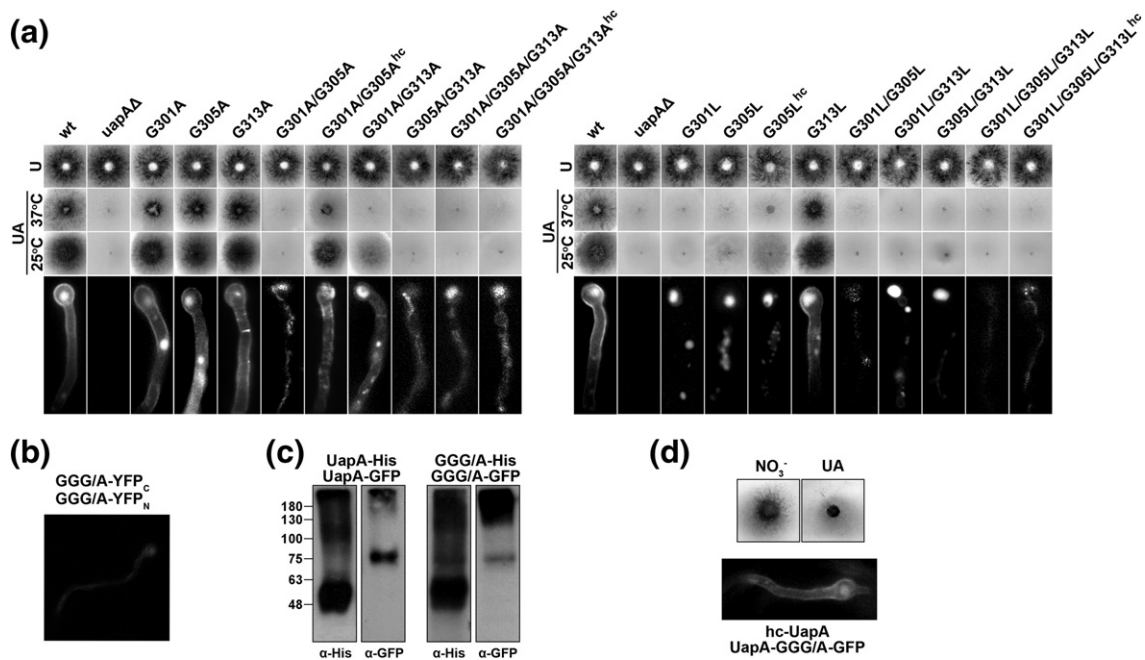


Fig. 9. Gly residues in TMS7 are critical for proper UapA dimerization, topology and turnover. (a) Growth tests and epifluorescence microscopy of mutants carrying Ala or Leu substitution in Gly residues of TMS7. (b) BiFC assay of UapA-GGG/A₃-YFP_N with UapA-GGG/A₃-YFP_C. No reconstituted YFP signal is detected. (c) Pull-down assays of protein extracts from strains co-expressing UapA-GGG/A₃-GFP with UapA-GGG/A₃-His and a wild-type relative control strain. (d) Growth tests and epifluorescence microscopy of a strain co-expressing UapA-GGG/A₃-GFP with multi-copy wild-type UapA (hc-UapA).

(Y. Alguel, B. Byrne and A. Cameron, personal communication).

One basic question to answer is how the cytoplasmic N-terminal DYDY₄₇ motif affects ER-exit. Does it interact with the packaging COPII machinery? We failed to detect an interaction with either Sec23 or Sec24 (results not shown). Alternatively,

the DYDY₄₇ motif might interact with a chaperone, specific for UapA packaging into COPII vesicles. ER membrane chaperones, involved in ER-exit of specific protein families, have been found in fungi [57–60]. In particular, Shr3p in *S. cerevisiae* is necessary for the correct association and concentrative ER-exit of all 18 amino acid transporters of the

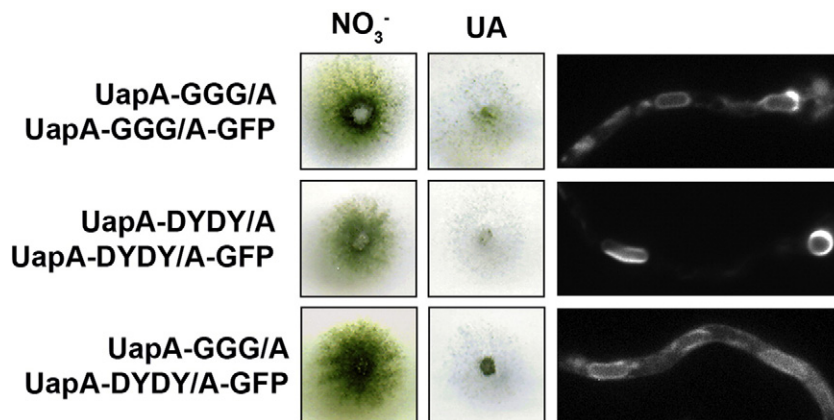


Fig. 10. Intragenic complementation of ER-retained mutants. Growth tests and epifluorescence microscopy of a strain co-expressing UapA-GGG/A₃ with UapA-DYDY/A₄-GFP. Control strains co-expressing either UapA-GGG/A₃ with UapA-GGG/A₃-GFP or UapA-DYDY/A₄ with UapA-DYDY/A₄-GFP are also shown. Partial re-localization of UapA-DYDY/A₄-GFP was observed only upon co-expression with UapA-GGG/A₃. Notice that there is no significant growth on UA, suggesting that both versions of UapA lack significant transport activity.

APC family. Interestingly, in the absence of Shr3p, amino acid transporters integrate in the ER membrane and fold correctly, but the monomers form aggregates and consequently fail to exit the ER membrane. However, we still cannot exclude that the cytoplasmic N-terminal DYDY₄₇ motif interacts with specific sequences of UapA, eliciting a topological effect, and thus promoting dimerization/oligomerization and ER-exit.

Our results are very similar to findings obtained on the role of oligomerization in the membrane trafficking of neurotransmitter transporters in mammals. Both the dopamine (DAT) [24–26] and serotonin (SERT) [23,28,30] transporters have been found to dimerize and eventually oligomerize into higher-order assemblies. The evidence for oligomerization in these cases comes from co-immunoprecipitation experiments, cross-linking and fluorescence resonance energy transfer but also from dominant-negative phenotypes obtained when mutants were co-expressed with wild-type proteins. Fluorescence resonance energy transfer signals in DAT were detected at the plasma membrane and in intracellular membrane compartments [25]. The similarity of our results with those of the neurotransmitter transporters is impressive. In both cases, wild-type oligomers are formed in the ER and then maintained both at the plasma membrane and during trafficking between the plasma membrane and endosomes. In addition, in both cases, co-expression of mutant and wild-type proteins led to negative (ER retention) or positive (plasma membrane localization) *in trans* sorting. Interestingly, it has also been proposed that oligomerization of DAT at the plasma membrane is reduced upon substrate binding and transport, and this in turn led to speculation that substrate-elicited endocytosis operates by loosening oligomerization. The evidence for that comes from a reduction in surface DAT determined by biotinylation and reduction in DAT oligomerization as assessed by cross-linking [27,29]. In UapA, the presence of substrates did not abolish oligomerization, as assessed by pull-down assays and the persistence of strong split-YFP fluorescent signals in endosomes and the vacuolar membrane upon endocytosis. Our findings do not answer the question whether UapA dimers further assemble into higher oligomeric complexes as seen for DAT and SERT.

Several logical assumptions suggest how oligomerization might have evolved to be a critical link among proper folding, quality control, ER-exit, membrane trafficking and turnover. Firstly, correct folding and maturation of a protein are required for oligomerization, ensuring that only correctly folded proteins enter the secretory pathway. Secondly, oligomerization can induce a conformational change that might increase the affinity for a specific ER membrane microdomain, which might then lead to further oligomerization owing to increased concentration in such a domain and eventually to concentrative ER-exit [19]. Thirdly,

homo-oligomerized cargoes could travel as highly specific membrane microdomains and remain so in their final membrane destination. This in turn provides a mechanistic solution to how specific transporters (or channels or receptors) could be sorted and turned over by endocytosis or direct sorting from the Golgi, in response to substrate excess or other specific physiological signals, without affecting the turnover of other transporters.

Materials and Methods

Media, strains, growth conditions and *A. nidulans* transformation

Standard complete and minimal media (MM) for *A. nidulans* were used[†]. *Escherichia coli* was grown on Luria-Bertani medium. Media and chemical reagents were obtained from Sigma-Aldrich (Life Science Chemilab SA, Hellas) or AppliChem (Bioline Scientific SA, Hellas). *A. nidulans* transformation was performed as described previously [60]. A Δ azgA Δ uapA Δ uapC::AfpyrG pabaA1 argB2 mutant strain [61] was the recipient strain in transformations with plasmids carrying differentially tagged wild-type or mutant versions of UapA (see below). Selection was based on complementation of the pabaA1 and argB2 genetic auxotrophies for *p*-aminobenzoic acid and arginine. Transformants expressing either single-copy or multi-copy plasmid integration events were identified by PCR and Southern analysis. A Δ uapA Δ uapC::AfpyrG Δ nkuaA::argB riboB2 pantoB100 pyroA4 mutant strain [36] was the recipient strain for generating “in locus” integrations of tagged uapA and prnB fusions (see below), based on complementation of the riboB2 and pantoB100 genetic auxotrophies for riboflavin and pantothenic acid, respectively. Growth tests were performed at 25 °C or 37 °C, at pH 6.8.

Standard nucleic acid manipulations

Genomic DNA extraction from *A. nidulans* was as described in Fungal Genetics Stock Center[‡]. Plasmid preparation from *E. coli* strains and DNA bands were purified from agarose gels using the Nucleospin Plasmid Kit and the Nucleospin ExtractII Kit according to the manufacturer's instructions (Macherey-Nagel, Lab Supplies Scientific SA, Hellas). DNA sequences were determined by VBC-Genomics (Vienna, Austria). Mutations were constructed by site-directed mutagenesis according to the instructions accompanying the QuikChange® Site-Directed Mutagenesis Kit (Agilent Technologies, Stratagene). Southern blot analysis was performed as described in Ref. [62]. [³²P]dCTP labeled molecules of uapA, argB or pabaA specific probes were prepared using a random hexanucleotide primer kit following the supplier's instructions (Takara Bio, Lab Supplies Scientific SA, Hellas) and purified on MicroSpin™ S-200 HR columns, following the supplier's instructions (Roche Diagnostics, Hellas). Labeled [³²P]dCTP (3000 Ci mmol⁻¹) was purchased from the Institute of Isotopes Co. Ltd, Miskolc, Hungary. Restriction enzymes were from Takara Bio (Lab Supplies Scientific SA, Hellas). Conventional PCR reactions were performed with KAPATaq DNA polymerase (Kapa Biosystems, Lab Supplies Scientific

SA, Hellas). Amplification of products and site-directed mutagenesis were performed with Kapa HiFi (Kapa Biosystems, Lab Supplies Scientific SA, Hellas).

Plasmid constructions

Plasmid pAN510 and derivatives pAN510exp, pAN510exp-GFP, pAN510-GFP and pBS-argB-alcA_p are described in previous articles [44,63–65]. These plasmids are derivatives from the original pAN510 plasmid [38,66] and were constructed by disrupting a XbaI site of the pBluescript polylinker and introducing a BamHI site next to the start codon of *uapA*, by site-directed mutagenesis. Given that there is a natural XbaI site after the stop codon of *uapA*, the *uapA* coding sequence could be exchanged by BamHI/XbaI double digestion. In pAN520exp, the *argB* sequence has been replaced by *pabaA* from pBS-pabaA [64]. The *alcA_p* 480-bp sequence was used to replace the native *uapA* promoter sequence in the derivative plasmids of the type pAN510. All point mutations were constructed by site-directed mutagenesis on plasmid pAN510-GFP or, in the case of multiple mutations, on already mutated versions of this plasmid. N-terminal truncations of UapA (Δ 3-30, Δ 3-42, Δ 3-62 and Δ 3-74) were constructed by introducing a BamHI restriction site at the desirable position and subcloning of the ORF (open reading frame) in pAN510exp-GFP. For BiFC analyses, the N-terminal half of yellow fluorescent protein (YFP_N; 154 amino acids of YFP) or the C-terminal half of YFP (YFP_C; 86 amino acids of YFP) was amplified from plasmids PDV7 and PDV8 [67] and cloned into pAN510exp, pAN510exp-alcA_p, pAN520exp or pAN520exp-alcA_p at the native XbaI site (XbaI/SpeI compatible end ligation), followed by cloning of the *uapA* ORF carrying the desirable mutations. The same approach (XbaI/SpeI compatible end ligation) was followed for the construction of plasmid pAN510exp-alcA_p-His. Plasmids expressing the UapA-YFP_N and PrmB-YFP_C were used as templates to generate gene replacement cassettes by PCR and were constructed by sequential cloning of the relevant ORFs together with approximately 1.5-kb upstream/downstream regions and the auxotrophic markers *riboB* (AN0670) and *pantoB* (AN1778), respectively.

Total protein extraction and Western blot analysis

Cultures for total protein extraction were grown in MM supplemented with nitrate at 25 °C for 16 h. Total protein extraction was performed as previously described [68]. Equal sample loading was estimated by Bradford assays and Coomassie staining. Total proteins (30 µg) were separated by SDS-PAGE [10% (w/v) polyacrylamide gel] and electrobotted (Mini PROTEAN™ Tetra Cell, Bio-Rad) onto PVDF membranes (Macherey-Nagel, Lab Supplies Scientific SA, Hellas) for immunodetection. The membrane was treated with 2% (w/v) non-fat dried milk and immunodetection was performed with a primary mouse anti-GFP monoclonal antibody (Roche Diagnostics, Hellas), a secondary goat anti-mouse IgG HRP-linked antibody (Cell Signaling Technology Inc., Biotek Scientific SA, Hellas) and a Penta-His HRP Conjugate antibody kit (Qiagen, SafeBlood BioAnalytica SA, Hellas). Blots were developed by the chemiluminescent method using the LumiSensor Chemiluminescent HRP Substrate kit (Genscript USA, Lab Supplies Scientific SA,

Hellas) and SuperRX Fuji medical X-ray films (FujiFILM Europe, Lab Supplies Scientific SA, Hellas).

Membrane-enriched extraction for purification

The membrane-enriched extraction protocol (adapted from Ref. [43]) was used prior to membrane protein purification by affinity chromatography. To increase protein yield, we performed the extraction procedure in 6–10 eppendorf tubes, containing mycelia of the same strain. The mycelia powder was resuspended in 2 mL of ice-cold extraction buffer (10 mM Tris-HCl, pH 7.5, 100 mM NaCl, 5 mM MgCl₂, 0.3 M sorbitol, 1 mM PMSF and 1 × Protease Inhibitor Cocktail), mixed by vortexing and incubated on ice for 20–30 min. The samples were then centrifuged for 3 min, at 3000 rpm, 4 °C, to remove cell debris and the supernatants were transferred in pre-frozen eppendorf tubes. Membrane proteins were then precipitated by centrifuging the samples for 1 h at 13,000 rpm, 4 °C. The pellets were resuspended in 80–100 µL of ice-cold solubilization buffer. The suspensions were collected in eppendorf tubes and solubilized, as described below.

Purification of membrane proteins and affinity chromatography

UapA purification was performed by combining affinity chromatography of a His-tagged recombinant version, UapA-His₁₀, with gel filtration chromatography. The procedure followed is an adaptation of the method described in Ref. [43]. Prior to chromatographic purification of UapA-His₁₀, crude membrane protein extracts are solubilized by resuspending in solubilization buffer [50 mM NaH₂PO₄/Na₂HPO₄, pH 8.0, 150 mM NaCl, 1% (w/v) dodecyl-β-D-maltoside (DDM), 1 mM PMSF and 1 × Protease Inhibitor Cocktail]. The sample was stirred gently for 30 min on ice and then centrifuged for 20 min at 12,000g, 4 °C, to separate the solubilized from the insoluble proteins. The supernatant (solubilized proteins) was then transferred to a pre-frozen eppendorf tube and glycerol was added to a final concentration of 20% (v/v) and gently mixed. The detergent-solubilized protein sample was stored at –80 °C for further use or loaded directly onto Protino Ni-NTA Columns (Macherey-Nagel GmbH) for purification. The mobile phase was delivered in a consistent flow rate of 1 mL/min via a pump. The column was first equilibrated with 10–20 column volumes of Ni-column wash buffer [50 mM NaH₂PO₄, pH 8.0, 300 mM NaCl, 0.01% (w/v) DDM and 1 mM PMSF], containing 10 mM imidazole. A total of 1–4 mg of protein in 1 mL of detergent solubilization buffer were applied to the column and 2.5 mL of the flow-through was collected and put on ice (fraction f₀). The column was washed abundantly (10–20 column volumes) with wash buffer containing 20 mM imidazole and subsequently with another containing 50 mM imidazole to remove unbound and loosely bound molecules. A total of 2.5 mL of each eluent were collected and put on ice (fractions f₂₀ and f₅₀). Bound protein was eluted with increasing concentrations of imidazole in the column wash buffer (250 mM, 350 mM and 500 mM) and 2.5 mL of each eluent was collected and put on ice (fractions f₂₅₀, f₃₅₀ and f₅₀₀). The column was washed abundantly with the 500 mM imidazole wash buffer and filled with 30% (v/v) EtOH before storing at 4 °C. Desalting and concentration of purified

proteins (UapA-His₁₀) was achieved by gel filtration in Sephadex G-25 columns. A total of 2.5 mL of each fraction eluted from the Ni-NTA column were loaded onto the Sephadex column, which was previously washed abundantly with distilled water. After the sample volume had completely entered the column, 3.5 mL of sterile distilled water was added to the column and the protein was eluted and frozen at -80°C . The frozen protein samples were then concentrated by overnight lyophilization. The freeze-dried samples were resuspended in a buffer containing 50 mM NaH₂PO₄/Na₂HPO₄, 10% glycerol, 0.1% (w/v) DDM, 1 mM PMSF and 1× Protease Inhibitor Cocktail, adjusted to pH 7.5 and analyzed electrophoretically and immunologically.

Kinetic analysis

[³H]xanthine (33 Ci mmol⁻¹; Moravex Biochemicals, California, USA) uptake in MM was assayed in germinating conidiospores of *A. nidulans* concentrated at 10⁷ conidiospores/100 μL, at 37 °C, pH 6.8, as recently described in detail [69]. All transport assays were carried out in at least three independent experiments, with three replicates for each concentration or time point. Standard deviation was <20%.

Epifluorescence microscopy

Samples for standard epifluorescence microscopy were prepared as previously described [35,36]. In brief, germlings incubated on coverslips in liquid MM supplemented with NaNO₃ as nitrogen source for 12–14 h at 25 °C were observed on an Axioplan Zeiss phase contrast epifluorescent microscope and the resulting images were acquired with a Zeiss-MRC5 digital camera using the AxioVs40 V4.40.0 software. Image processing, contrast adjustment and color combining were made using the Adobe Photoshop CS4 Extended version 11.0.2 software or the ImageJ software. Images were converted to RGB and annotated using Photoshop CS4 before being saved to TIFF. For inverted fluorescence microscopy, germlings were incubated in sterile 35-mm micro-dishes, high glass bottom (*ibidi*, Germany) in liquid MM supplemented with NaNO₃ as nitrogen source for 16–18 h at 25 °C. Images were obtained with an AxioCam HR R3 camera using the Zen lite 2012 software either as single images or in stacks of 10–12 optical sections along z-axis with a Z step size at 0.31 μm. Contrast adjustment, area selection and color combining were made using the Zen 2012 software. Images exported as tiffs were annotated and further processed in Adobe Photoshop CS4 Extended version 11.0.2 software for brightness adjustment, rotation and alignment. A desaturated and inverted version of the image was also created in each case, so as to achieve better visualization.

Static light-scattering measurements of purified UapA

UapA-G411VΔ1-11, a thermostabilised version of the UapA, was expressed and isolated as described previously [37]. The oligomeric state of the UapA-G411VΔ1-11 construct at a detected protein concentration of 1.4 mg/mL in sample buffer (20 mM Tris-HCl, pH 7.5, 150 mM NaCl, 5% glycerol, 500 mM xanthine and 0.03% DDM) was

assessed with a Malvern Viscotek TDMax Tetra detection system, including static light scattering, UV and refractive index detectors, connected downstream of a Superdex-200 10/30 gel-filtration column previously equilibrated in sample buffer. The protein is initially separated on the gel-filtration column prior to further analysis. The data were analyzed with the Omnic software (Malvern) following the manufacturer's protocols and used to calculate the MW of the protein particles in the individual fractions eluting from the column. In this case, the detergent micelles present in the sample contribute to the size of the protein particles. The system was calibrated first with buffer containing DDM detergent alone at the same concentration as the test sample [0.03% (w/v) DDM_{LA}] and the size of the detergent micelles was calculated. This is then subtracted from the MW of the protein-detergent complex to provide an accurate assessment of the size of the protein particles.

Selection of genetic suppressors

UV exposure conditions used for the mutagenesis of the strain expressing UapA-Y47A were determined based on a specifically constructed cell survival curve. According to the resulting cell survival curve, the time for achieving >98% lethality in 10⁷ conidiospores, which was used for this work, was estimated at 4 min 30 s. UV exposure of conidiospore suspensions in 0.01% Tween in Petri dishes was performed at a standard distance of 20 cm from an Osram HNS30 UV-B/C lamp. Mutagenized conidiospores were plated in standard MM supplemented with 0.5 mM uric acid as sole nitrogen source and necessary vitamins. Suppressors appeared as distinct well conidiating colonies after 7 days of incubation at 25 °C.

Acknowledgments

We are grateful to Joseph Strauss for hosting in his laboratory and supporting Sotiris Amillis during the systematic mutational analysis of the UapA. We thank Anna Vlanti for assisting in the construction of some mutants. We also thank Vassilis Bitsikas for critical comments. Olga Martzoukou and work in the laboratory of George Diallinas were supported by a research grant from Fondation Santé. Mayia Karachaliou was supported by the European Union (European Social Fund) and Greek national funds through the Operational Program "Education and Lifelong Learning" of the National Strategic Reference Framework Research Funding Program: Heracleitus II, Investing in Knowledge Society through the European Social Fund, Investing in Knowledge Society through the European Social Fund. Work in the laboratory of Bernadette Byrne and James Leung was supported by the European Community's Seventh Framework Program FP7/2007-2013 under Grant Agreement No. HEALTH-F4-2007-201924, EDICT Consortium and Biotechnology and Biological Sciences Research Council grant BB/K017292/1.

Appendix A. Supplementary data

Supplementary data to this article can be found online at <http://dx.doi.org/10.1016/j.jmb.2015.05.021>.

Received 5 March 2015;

Received in revised form 27 May 2015;

Accepted 28 May 2015

Available online 3 June 2015

Keywords:

transport;
membrane sorting;
trafficking;
bimolecular fluorescence;
endocytosis

† Media and supplemented auxotrophies were at the concentrations given in <http://www.fgsc.net>.

‡ <http://www.fgsc.net>.

Abbreviations used:

BiFC, bimolecular fluorescence complementation; MW, molecular weight; MM, minimal media; DDM, dodecyl- β -D-maltoside.

References

- [1] Nyathi Y, Wilkinson BM, Pool MR. Co-translational targeting and translocation of proteins to the endoplasmic reticulum. *Biochim Biophys Acta* 2013;1833:2392–402.
- [2] D'Arcangelo JG, Stahmer KR, Miller EA. Vesicle-mediated export from the ER: COPII coat function and regulation. *Biochim Biophys Acta* 2013;1833:2464–72.
- [3] Barlowe C. Signals for COPII-dependent export from the ER: what's the ticket out? *Trends Cell Biol* 2003;13:295–300.
- [4] Sato K, Nakano A. Mechanisms of COPII vesicle formation and protein sorting. *FEBS Lett* 2007;581:2076–82.
- [5] Fath S, Mancias JD, Bi X, Goldberg J. Structure and organization of coat proteins in the COPII cage. *Cell* 2007;129:1325–36.
- [6] Budnik A, Stephens DJ. ER exit sites-localization and control of COPII vesicle formation. *FEBS Lett* 2009;583:3796–803.
- [7] Copic A, Latham CF, Horlbeck MA, D'Arcangelo JG, Miller EA. ER cargo properties specify a requirement for COPII coat rigidity mediated by Sec13p. *Science* 2012;335:1359–62.
- [8] Gillon AD, Latham CF, Miller EA. Vesicle-mediated ER export of proteins and lipids. *Biochim Biophys Acta* 2012;1821:1040–9.
- [9] Ruggiano A, Foresti O, Carvalho P. Quality control: ER-associated degradation: protein quality control and beyond. *J Cell Biol* 2014;204:869–79.
- [10] Stolz A, Ernst A, Dikic I. Cargo recognition and trafficking in selective autophagy. *Nat Cell Biol* 2014;16:495–501.
- [11] Wang X, Matteson J, An Y, Moyer B, Yoo JS, Bannykh S, et al. COPII-dependent export of cystic fibrosis transmembrane conductance regulator from the ER uses a di-acidic exit code. *J Cell Biol* 2004;167:65–74.
- [12] Renard HF, Demaegd D, Guerriat B, Morsomme P. Efficient ER exit and vacuole targeting of yeast Sna2p require two tyrosine-based sorting motifs. *Traffic* 2010;11:931–46.
- [13] Dong C, Nichols CD, Guo J, Huang W, Lambert NA, Wu G. A triple arg motif mediates α (2B)-adrenergic receptor interaction with Sec24C/D and export. *Traffic* 2012;13:857–68.
- [14] Otsu W, Kurooka T, Otsuka Y, Sato K, Inaba M. A new class of endoplasmic reticulum export signal PhiXPhiXPhi for transmembrane proteins and its selective interaction with Sec24C. *J Biol Chem* 2013;288:18521–32.
- [15] Guo Y, Sirkis DW, Schekman R. Protein Sorting at the trans-Golgi Network. *Annu Rev Cell Dev Biol* 2014;30:169–206.
- [16] Russell C, Stagg SM. New insights into the structural mechanisms of the COPII coat. *Traffic* 2010;11:303–10.
- [17] Sato K, Nakano A. Oligomerization of a cargo receptor directs protein sorting into COPII-coated transport vesicles. *Mol Biol Cell* 2003;14:3055–63.
- [18] Sato K, Nakano A. Emp47p and its close homolog Emp46p have a tyrosine-containing endoplasmic reticulum exit signal and function in glycoprotein secretion in *Saccharomyces cerevisiae*. *Mol Biol Cell* 2002;13:2518–32.
- [19] Springer S, Malkus P, Borchert B, Wellbrock U, Duden R, Schekman R. Regulated oligomerization induces uptake of a membrane protein into COPII vesicles independent of its cytosolic tail. *Traffic* 2014;15:531–45.
- [20] Lu X, Zhang Y, Shin YK. Supramolecular SNARE assembly precedes hemifusion in SNARE-mediated membrane fusion. *Nat Struct Mol Biol* 2008;5:700–6.
- [21] Van Craenenbroeck K. GPCR oligomerization: contribution to receptor biogenesis. *Subcell Biochem* 2012;63:43–65.
- [22] Wu G. Identification of endoplasmic reticulum export motifs for G protein-coupled receptors. *Methods Enzymol* 2013;521:189–202.
- [23] Kilic F, Rudnick G. Oligomerization of serotonin transporter and its functional consequences. *Proc Natl Acad Sci U S A* 2000;97:3106–11.
- [24] Hastrup H, Sen N, Javitch JA. The human dopamine transporter forms a tetramer in the plasma membrane: cross-linking of a cysteine in the fourth transmembrane segment is sensitive to cocaine analogs. *J Biol Chem* 2003;278:45045–8.
- [25] Sorkina T, Doolen S, Galperin E, Zahniser NR, Sorkin A. Oligomerization of dopamine transporters visualized in living cells by fluorescence resonance energy transfer microscopy. *J Biol Chem* 2003;278:28274–83.
- [26] Torres GE, Carneiro A, Seamans K, Fiorentini C, Sweeney A, Yao WD, et al. Oligomerization and trafficking of the human dopamine transporter. Mutational analysis identifies critical domains important for the functional expression of the transporter. *J Biol Chem* 2003;278:2731–9.
- [27] Chen N, Reith ME. Substrates dissociate dopamine transporter oligomers. *J Neurochem* 2008;105:910–20.
- [28] Fjorback AW, Pla P, Müller HK, Wiborg O, Saudou F, Nyengaard JR. Serotonin transporter oligomerization documented in RN46A cells and neurons by sensitized acceptor emission FRET and fluorescence lifetime imaging microscopy. *Biochem Biophys Res Commun* 2009;380:724–8.
- [29] Li Y, Cheng SY, Chen N, Reith ME. Interrelation of dopamine transporter oligomerization and surface presence as studied with mutant transporter proteins and amphetamine. *J Neurochem* 2010;114:873–85.
- [30] Anderluh A, Klotzsch E, Reismann AW, Brameshuber M, Kudlacek O, Newman AH, et al. Single molecule analysis reveals coexistence of stable serotonin transporter monomers and oligomers in the live cell plasma membrane. *J Biol Chem* 2014;289:4387–99.
- [31] De Zutter JK, Levine KB, Deng D, Carruthers A. Sequence determinants of GLUT1 oligomerization: analysis by

- homology-scanning mutagenesis. *J Biol Chem* 2013;288:20734–44.
- [32] Diallinas G, Gournas C. Structure–function relationships in the nucleobase-ascorbate transporter (NAT) family: lessons from model microbial genetic systems. *Channels (Austin)* 2008;2:363–72.
- [33] Gournas C, Papageorgiou I, Diallinas G. The nucleobase-ascorbate transporter (NAT) family: genomics, evolution, structure–function relationships and physiological role. *Mol Biosyst* 2008;4:404–16.
- [34] Kosti V, Lambrinidis G, Myriantopoulos V, Diallinas G, Mikros E. Identification of the substrate recognition and transport pathway in a eukaryotic member of the nucleobase-ascorbate transporter (NAT) family. *PLoS ONE* 2012;7:e41939.
- [35] Gournas C, Amillis S, Vlanti A, Diallinas G. Transport-dependent endocytosis and turnover of a uric acid-xanthine permease. *Mol Microbiol* 2010;75:246–60.
- [36] Karachaliou M, Amillis S, Evangelinos M, Kokotos AC, Yaleis V, Diallinas G. The arrestin-like protein ArtA is essential for ubiquitination and endocytosis of the UapA transporter in response to both broad-range and specific signals. *Mol Microbiol* 2013;88:301–17.
- [37] Leung J, Cameron AD, Diallinas G, Byrne B. Stabilizing the heterologously expressed uric acid-xanthine transporter UapA from the lower eukaryote *Aspergillus nidulans*. *Mol Membr Biol* 2013;30:32–42.
- [38] Koukaki M, Vlanti A, Goudela S, Pantazopoulou A, Gioule H, Tournaviti S, et al. The nucleobase-ascorbate transporter (NAT) signature motif in UapA defines the function of the purine translocation pathway. *J Mol Biol* 2005;350:499–513.
- [39] Diallinas G, Scazzocchio C. A gene coding for the uric acid-xanthine permease of *Aspergillus nidulans*: inactivational cloning, characterization, and sequence of a *cis*-acting mutation. *Genetics* 1989;122:341–50.
- [40] Hu CD, Chinenov Y, Kerppola TK. Visualization of interactions among bZIP and Rel family proteins in living cells using bimolecular fluorescence complementation. *Mol Cell* 2002;9:789–98.
- [41] Vangelatos I, Vlachakis D, Sophianopoulou V, Diallinas G. Modelling and mutational evidence identify the substrate binding site and functional elements in APC amino acid transporters. *Mol Membr Biol* 2009;26:356–70.
- [42] Felenbok B. The ethanol utilization regulon of *Aspergillus nidulans*: the alcA-alcR system as a tool for the expression of recombinant proteins. *J Biotechnol* 1991;17:11–7.
- [43] Lemuh ND, Diallinas G, Frilingos S, Mermelekas G, Karagouni AD, Hatzinikolaou DG. Purification and partial characterization of the xanthine-uric acid transporter (UapA) of *Aspergillus nidulans*. *Protein Expr Purif* 2009;63:33–9.
- [44] Pantazopoulou A, Lemuh ND, Hatzinikolaou DG, Drevet C, Cecchetto G, Scazzocchio C, et al. Differential physiological and developmental expression of the UapA and AzgA purine transporters in *Aspergillus nidulans*. *Fungal Genet Biol* 2007;44:627–40.
- [45] Amillis S, Kosti V, Pantazopoulou A, Mikros E, Diallinas G. Mutational analysis and modeling reveal functionally critical residues in transmembrane segments 1 and 3 of the UapA transporter. *J Mol Biol* 2011;411:567–80.
- [46] Vlanti A, Amillis S, Koukaki M, Diallinas G. A. A novel-type substrate-selectivity filter and ER-exit determinants in the UapA purine transporter. *J Mol Biol* 2006;357:808–19.
- [47] Lu F, Li S, Jiang Y, Jiang J, Fan H, Lu G, et al. Structure and mechanism of the uracil transporter UraA. *Nature* 2011;472:243–6.
- [48] Kleiger G, Grothe R, Mallick P, Eisenberg D. GXXXG and AXXXA: common alpha-helical interaction motifs in proteins, particularly in extremophiles. *Biochemistry* 2002;41:5990–7.
- [49] Senes A, Engel DE, DeGrado WF. Folding of helical membrane proteins: the role of polar, GxxxG-like and proline motifs. *Curr Opin Struct Biol* 2004;14:465–79.
- [50] Mueller BK, Subramaniam S, Senes A. A frequent, GxxxG-mediated, transmembrane association motif is optimized for the formation of interhelical C^α-H hydrogen bonds. *Proc Natl Acad Sci U S A* 2014;111:E888–95.
- [51] Haider AJ, Briggs D, Self TJ, Chilvers HL, Holliday ND, Kerr ID. Dimerization of ABCG2 analysed by bimolecular fluorescence complementation. *PLoS ONE* 2011;6:e25818.
- [52] Chang MH, Chen AP, Romero MF. NBCE1A dimer assemble visualized by bimolecular fluorescence complementation. *Am J Physiol Renal Physiol* 2014;306:F672–80.
- [53] Lasry I, Golan Y, Berman B, Amram N, Glaser F, Assaraf YG. In situ dimerization of multiple wild type and mutant zinc transporters in live cells using bimolecular fluorescence complementation. *J Biol Chem* 2014;289:7275–92.
- [54] Li N, Cui Z, Fang F, Lee JY, Ballatori N. Heterodimerization, trafficking and membrane topology of the two proteins, Ost alpha and Ost beta, that constitute the organic solute and steroid transporter. *Biochem J* 2007;407:363–72.
- [55] McFarlane HE, Shin JJ, Bird DA, Samuels AL. Arabidopsis ABCG transporters, which are required for export of diverse cuticular lipids, dimerize in different combinations. *Plant Cell* 2010;22:3066–75.
- [56] Salazar K, Cerda G, Martínez F, Sarmiento JM, González C, Rodríguez F, et al. SVCT2 transporter expression is post-natally induced in cortical neurons and its function is regulated by its short isoform. *J Neurochem* 2014;130:693–706.
- [57] Gilstring CF, Melin-Larsson M, Ljungdahl PO. Shr3p mediates specific COPII coatomer-cargo interactions required for the packaging of amino acid permeases into ER-derived transport vesicles. *Mol Biol Cell* 1999;10:3549–65.
- [58] Martínez P, Ljungdahl PO. The SHR3 homologue from *S. pombe* demonstrates a conserved function of ER packaging chaperones. *J Cell Sci* 2000;113:4351–62.
- [59] Kota J, Ljungdahl PO. Specialized membrane-localized chaperones prevent aggregation of polytopic proteins in the ER. *J Cell Biol* 2005;168:79–88.
- [60] Erpapazoglou Z, Kafasla P, Sophianopoulou V. The product of the SHR3 orthologue of *Aspergillus nidulans* has restricted range of amino acid transporter targets. *Fungal Genet Biol* 2006;43:222–33.
- [61] Koukaki M, Giannoutsou E, Karagouni A, Diallinas G. A novel improved method for *Aspergillus nidulans* transformation. *J Microbiol Methods* 2003;55:687–95.
- [62] Sambrook J, Russell DW. *Molecular cloning: a laboratory manual*. Cold Spring Harbor, New York: Cold Spring Harbor Laboratory Press; 2001.
- [63] Diallinas G, Valdez J, Sophianopoulou V, Rosa A, Scazzocchio C. Chimeric purine transporters of *Aspergillus nidulans* define a domain critical for function and specificity conserved in bacterial, plant and metazoan homologues. *EMBO J* 1998;17:3827–37.
- [64] Vlanti A, Diallinas G. The *Aspergillus nidulans* FcyB cytosine-purine scavenger is highly expressed during germination and in reproductive compartments and is downregulated by endocytosis. *Mol Microbiol* 2008;68:959–77.
- [65] Papageorgiou I, Gournas C, Vlanti A, Amillis S, Pantazopoulou A, Diallinas G. Specific interdomain synergy

- in the UapA transporter determines its unique specificity for uric acid among NAT carriers. *J Mol Biol* 2008;382:1121–35.
- [66] Gorfinkiel L, Diallinas G, Scazzocchio C. Sequence and regulation of the *uapA* gene encoding a uric acid-xanthine permease in the fungus *Aspergillus nidulans*. *J Biol Chem* 1993;268:23376–81.
- [67] Takeshita N, Higashitsuji Y, Konzack S, Fischer R. Apical sterol-rich membranes are essential for localizing cell end markers that determine growth directionality in the filamentous fungus *Aspergillus nidulans*. *Mol Biol Cell* 2008;19:339–51.
- [68] Galanopoulou K, Scazzocchio C, Galinou ME, Liu W, Borbolis F, Karachaliou M, et al. Purine utilization proteins in the Eurotiales: cellular compartmentalization, phylogenetic conservation and divergence. *Fungal Genet Biol* 2014;69:96–108.
- [69] Kryptou E, Diallinas G. Transport assays in filamentous fungi: kinetic characterization of the UapC purine transporter of *Aspergillus nidulans*. *Fungal Genet Biol* 2014;63:1–8.